Low microRNA150 expression is associated with activated carcinogenic pathways and a poor prognosis in patients with breast cancer

SAN-QI AN[1,2*], KE HE[1*], FEI LIU[1], QIAN-SHAN DING[3], YAN-LI WEI[1,4], ZHENG-LIN XIA[1], XIAO-PENG DUAN[1], RUI HUANG[1], BO-WEI LI[1], HAI-HE WANG[1,4], YU TIAN[5], GUO-AN XIANG[1] and WEN-XING LI[6,7]

[1]Department of General Surgery, Guangdong Second Provincial General Hospital, Guangzhou, Guangdong 510317; [2]Biosafety Level-3 Laboratory, Life Sciences Institute and Guangxi Key Laboratory of AIDS Prevention and Treatment and Guangxi Collaborative Innovation Center for Biomedicine, Guangxi Medical University, Nanning, Guangxi 530021; [3]Department of Gastroenterology, Renmin Hospital of Wuhan University, Wuhan, Hubei 430060; [4]Center for Stem Cell Biology and Tissue Engineering, Key Laboratory of Ministry of Education, Sun Yat-sen University, Guangzhou, Guangdong 510080; [5]Henan Cancer Hospital, Zhengzhou, Henan 450000; [6]Key Laboratory of Animal Models and Human Disease Mechanisms, Kunming Institute of Zoology, Chinese Academy of Sciences, Kunming, Yunnan 650223; [7]Kunming College of Life Science, University of Chinese Academy of Sciences, Kunming, Yunnan 650204, P.R. China

Received April 5, 2020; Accepted October 15, 2020

DOI: 10.3892/or.2021.7945

Abstract. Breast cancer is the most common type of cancer amongst women worldwide, and numerous microRNAs (miRNAs/miRs) are involved in the initiation and progression of breast cancer. The aim of the present study was to identify hub miRNAs and determine the underlying mechanisms regulated by these miRNAs in breast cancer. Breast invasive carcinoma transcriptome data (including mRNAs and miRNAs), and clinical data were acquired from The Cancer Genome Atlas database. Differential gene expression analysis, co-expression network analysis, gene set enrichment analysis (GSEA) and prognosis analysis were used to screen the hub miRNAs and explore their functions. Functional experiments were used to determine the underlying mechanisms of the hub miRNAs in breast cancer cells. The results revealed that low miR150 expression predicted a more advanced disease stage, and was associated with a less favorable prognosis. Through the combined use of five miRNA-target gene prediction tools, 31 potential miR150 target genes were identified. GSEA revealed that low miR150 expression was associated with the upregulation of several cancer-associated signaling pathways, and the downregulation of several tumor suppressor genes. Furthermore, miR150 independently affected overall survival in patients, and interacted with its target genes to indirectly affect overall and disease-free survival. Functional experiments demonstrated that miR150 positively regulated B and T lymphocyte attenuator (BTLA), and the downregulation of miR150 and BTLA combined promoted cell migration. In conclusion, the present study revealed that low miR150 expression was associated with less favorable clinical features, upregulation of several carcinogenic signaling pathways, and poor patient survival. Additionally, a miR150-BTLA axis was suggested to regulate cell viability and migration.

Correspondence to: Dr Guo-An Xiang, Department of General Surgery, Guangdong Second Provincial General Hospital, 466 Xingang Middle Road, Haizhu, Guangzhou, Guangdong 510317, P.R. China
E-mail: guoan_66@163.com

Dr Wen-Xing Li, Key Laboratory of Animal Models and Human Disease Mechanisms, Kunming Institute of Zoology, Chinese Academy of Sciences, 32 Jiaochang East Road, Wuhua, Kunming, Yunnan 650223, P.R. China
E-mail: liwenxing2016@gmail.com

*Contributed equally

Abbreviations: BRCA, breast invasive carcinoma; TCGA, The Cancer Genome Atlas; GENIE3, Gene Network Inference with Ensemble of trees; GSEA, gene set enrichment analysis; KEGG, Kyoto Encyclopedia of Genes and Genomes; OS, overall survival; DFS, disease-free survival; FDR, false discovery rate

Key words: breast cancer, prognosis, microRNA150, B and T lymphocyte attenuator, cell migration

Introduction

Breast cancer is the most common type of cancer in women worldwide (1). In China, the incidence of breast cancer has increased in recent decades, and it is estimated to account for 15% of all newly diagnosed cases of cancer in women (1). The Tumor-Node-Metastasis staging system (2), histological grade, lymph node status, estrogen receptor (ER), progestogen receptor (PR) and human epidermal growth factor receptor 2 (HER2) status are commonly used biological indicators for breast

cancer diagnosis, treatment and prognosis assessment (2). Although these indicators have consistent clinical outcomes in several patients with breast cancer, other patients with a similar combination of these features can respond differently to treatment, and have a variable prognosis status (3). Therefore, novel biomarkers and methods are required to improve the accuracy of diagnosis and prognosis, and to facilitate the determination of the most appropriate treatment for patients with breast cancer on an individual basis.

MicroRNAs (miRNAs/miRs) are RNAs of ~22 nucleotides that primarily function in regulating gene expression via several mechanisms (4). Dysregulation of miRNAs is involved in the initiation and progression of several types of cancer, including breast cancer (5-9). Studies have demonstrated that several upregulated miRNAs can regulate numerous functional genes and influence tumor development or metastasis (5-7). Upregulation of miR21, miR27a, miR155 and miR206 expression has been detected in breast tumor tissues and several human breast cancer cell lines, and was demonstrated to serve a crucial role in all phases of breast cancer pathogenesis (5). The expression levels of Let-7 family members are downregulated in breast cancer, and low let-7 expression is associated with a less favorable prognosis (6). As a driver of metastasis, miR10b binds to Homeobox D10, and enhances cell migration and invasion (7). Due to their evolutionary conservation and relatively easy means of detection in tumor biopsies, several miRNAs have been proposed as promising biomarkers of breast cancer (8). Numerous studies have revealed that the combination of several prognosis-associated miRNAs may be used to differentiate breast tumors from normal breast tissues with a high degree of accuracy (8,9). However, these miRNA markers are typically screened from a small group of patients (<100), and thus require validation in larger datasets and cohorts to verify the applicability in the general population.

The interaction between miRNAs and their target genes affects multiple biological functions and patient prognosis in patients with breast cancer (10). The determination of the binding characteristics to target mRNAs by miRNAs is important in defining their functions. Several computational algorithms have been developed and implemented as software tools for miRNA target prediction (11-15). The major features of these prediction tools are the sequence composition (seed match), conservation and thermodynamic stability (free energy) (16). Considering that each algorithm has its limitations, the combined use of these tools should result in more accurate results (16). The aim of the present study was to determine the hub miRNAs in breast cancer using multiple bioinformatics approaches combined with target gene prediction to explore the potential carcinogenic mechanisms of the identified miRNAs.

Materials and methods

Breast cancer data collection. Breast cancer transcriptome data (including mRNA and miRNA expression) and clinical data were acquired from The Cancer Genome Atlas (TCGA) database (cancergenome.nih.gov/). Non-solid tumor samples or patients who lacked prognostic data were removed. The filtered female samples contained 1,076 breast tumor and 104 adjacent normal tissues [TCGA-breast invasive carcinoma (BRCA)]. All samples were RNA sequenced using the Illumina HiSeq 2000 platform (version 2). mRNA expression was normalized using the RNA-sequencing by expectation maximization method, and miRNA expression was normalized using the reads per million miRNA mapped method (https://www.cancer.gov/tcga). Considering that the high imbalance in the numbers of breast tumor and adjacent normal tissues may introduce some bias in the expression analysis of miR150, a comprehensive analysis was conducted from multiple perspectives. The validation datasets GSE22220 (17) and GSE40267 (18) were downloaded from the Gene Expression Omnibus database (ncbi.nlm.nih.gov/geo/). However, there is no information on hormone receptor status in the validation sets.

Data pre-processing and differential expression analysis. R version 3.4.0 (https://www.r-project.org/) was used to perform data pre-processing. The mRNAs and miRNAs with a median expression value >0 in all samples were selected, and those with no expression in >50% of the samples were removed. All mRNA and miRNA expression values were $\log_2$-transformed. Differentially expressed mRNAs and miRNAs were calculated using the empirical Bayes method using the limma package (19). Upregulated and downregulated mRNAs and miRNAs were defined as $\log_2$fold change (FC)≥|1|. A false discovery rate (FDR)-corrected P≤0.05 was considered to indicate a statistically significant difference.

Construction of the miRNA-mRNA co-expression network. Gene Network Inference with Ensemble of trees (GENIE3) (20) was used to construct the miRNA-mRNA co-expression network. The combined mRNA and miRNA expression matrix was used as the input data, and the network was constructed using the default parameters in GENIE3. The top 10,000 miRNA-mRNA interactions were extracted from the original output, and the network was visualized using Cytoscape version 3.4.0 (cytoscape.org/). The NetworkAnalyzer function in Cytoscape was used to analyze the network.

miRNA target gene prediction. A total of five web-based target prediction tools, including microRNA (11), miRTarBase (12), mmmRNA (13), miRGate (14) and miRDB (15), were used to predict the target genes of the given miRNAs, and the commonly predicted genes were considered the miRNA target genes. The univariate linear model was used to analyze the linear correlation between miRNAs and the predicted target genes. Pearson's correlation coefficients were calculated between miRNAs and their predicted target genes. An absolute value of the correlation coefficient ≥0.1 and an FDR-corrected P≤0.05 were considered to indicate a statistically significant difference.

miRNA, clinicopathological features and prognostic analysis. The results for categorical variables, including ethnicity, ER status, PR status, HER2 status and stage [according to the American Joint Committee on Cancer staging manual (2), are presented as the number and percentage of cases. Continuous variables, including age at diagnosis, copy number alterations, number of lymph nodes examined, mutation count, disease-free survival (DFS) in months and overall survival (OS) in months, are presented as the mean ± standard deviation. The means

of continuous variables in two groups were compared using unpaired Student's t-tests, and the prevalence of categorical variables was compared using a χ^2 test. Due to the small sample size in stage and ethnicity, the comparisons were performed using a χ^2 test with Yates' continuity correction and Fisher's exact test. Pearson's correlation analysis was used to analyse the correlation between disease stage and miR150 expression. The unitary linear regression model was used to assess the associations between miRNAs and clinicopathological features. All survival analyses were performed using the survival package in R. Kaplan-Meier survival curve analysis was used to exhibit the prognostic differences between two groups. The univariate Cox proportional hazards model was used to determine the effect of the miRNAs and clinical features on patient survival status. The multivariate Cox proportional hazards model was used to explore the independent effect of miRNAs on patient OS and DFS with adjusted related covariates. $P \leq 0.05$ was considered to indicate a statistically significant difference.

Gene set enrichment analysis (GSEA). GSEA was performed using javaGSEA Desktop Application version 2.2.4 (21). The gene set used in enrichment operations was the Kyoto Encyclopedia of Genes and Genomes (KEGG) gene sets version 6.0 (https://www.gsea-msigdb.org/gsea/index.jsp), which included 186 gene sets. The analytical parameters were set as follows: Gene sets containing <15 genes or >500 genes were excluded, a phenotype label was set as case vs. control, and the t-statistic mean of the genes was computed in each KEGG pathway using a permutation test with 1,000 replications. The upregulated pathways were defined by a normalized enrichment score (NES)>0, and the downregulated pathways were defined by a NES<0. Pathways with an FDR-corrected $P \leq 0.05$ were considered as significantly enriched.

Cell culture and antibodies. MDA-MB-231 and MCF7 cells were purchased from the American Type Culture Collection. All cells were maintained in RPMI 1640 medium supplemented with 10% FBS (both Gibco; Thermo Fisher Scientific, Inc.), 100 U/ml penicillin and 100 mg/ml streptomycin (Beyotime Institute of Biotechnology). The cells were cultured at 37˚C with 5% CO_2 in a humidified incubator. Antibodies against anti-rat B and T lymphocyte attenuator (BTLA) (1:500; cat. no. 250587) were purchased from Abbiotec, Inc., while antibodies against β-actin (1:1,000; cat. no. sc-130300) were purchased from Santa Cruz Biotechnology, Inc..

Overexpression and knockdown of miR150, and knockdown of BTLA. miR150 overexpression and knockdown were performed using liposome-mediated miRNA mimics and inhibitors transfection. Chemically modified hsa-miR150 mimics (5'-UCUCCCAACCCUUGUACCAGUG-3'), hsa-miR150 inhibitor (5'-CACUGGUACAAGGGUUGGGAGA-3'), scrambled miRNA mimics negative control (mimics NC; 5'-CACUGGUACAAGGGUUGGGAGA-3') and inhibitor NC (5'-CAGUACUUUUGUGUAGUACAA-3') were purchased from Guangzhou RiboBio Co., Ltd.. Small interfering RNAs (siRNAs) specific to human BTLA (si-BTLA forward, 5'-GGUAGAUGAUGGUAUUAUACU-3' and reverse, 5'-UAUAAUACCAUCAUCUACCUA-3') and non-targeting siRNA (si-NC, forward, 5'-UUCUCCGAACGUGUCACGUTT-3' and reverse, 5'-ACGUGACACGUUCGGAGAATT-3') were designed and synthesized by Shanghai GenePharma Co., Ltd. MDA-MB-231 and MCF7 cells were transfected using Lipofectamine® 2000 (Invitrogen; Thermo Fisher Scientific, Inc.) at 37˚C for 6 h according to the manufacturer's protocol with working concentrations of 20 nM for the inhibitors/mimics and 30 nM for the siRNAs. miR150 mimics and inhibitors were transfected into MDA-MB-231 cells. miR150 inhibitors were transfected into MCF7 cells. After 48 h of transfection, the cells were used for subsequent experiments.

Cell viability assay. For the cell viability assays, cells were counted and plated in 96-well plates (1,500 cells/well) 24 h after transfection with the modified oligonucleotides (miR150 mimics/inhibitors) or siRNA. Cell viability was determined using a Cell Counting Kit-8 (CCK-8) assay (Dojindo Molecular Technologies, Inc.) according to the manufacturer's protocol. CCK-8 reagent was added into the culture medium at the indicated time points (0, 24, 48 and 72 h) and incubated for 60 min. The absorbance was measured using a microplate reader at 450 nm. All experiments were performed in triplicate.

Reverse transcription-quantitative (RT-q)PCR. Total RNA was isolated from cell lines using an RNA isolation kit (Takara Bio, Inc.). Moloney murine leukemia virus (MMLV) reverse transcriptase (Takara Bio, Inc.; 1X 200 μl MMLV RT, 1 ml 5X First Strand Buffer and 500 μl 100 mM DTT) was used to synthesize the cDNA. A SYBR Green reaction system (Takara Bio, Inc.) was used to amplify the cDNA. The thermocycling conditions were 95˚C for 10 min, followed by 40 cycles of 95˚C for 15 sec and 60˚C for 1 min. The differences in miR150 RNA expression were normalized to the levels of U6. The sequences of the PCR primers were: miR150 sense, 5'-CTCAACTGGTGTCGTGGAGTCGGCAATTCAGTTGAGCACTGGTA-3' and antisense, 5'-ACACTCCAGCTGGGTCTCCCAACCCTTGTA-3'; BTLA sense, 5'-ATCCCAGATGCTACCAATGC-3' and antisense, 5'-TTGGGAGTTTGTCCTGGAAC-3'; U6 sense, 5'-CCGTATGACCTCCTTCCACAGA-3' and antisense, 5'-TCTGTCCACCTCTGAAACCAGG-3'; and GAPDH sense, 5'-TGTTCGTCATGGGTGTGAAC-3' and antisense, 5'-ATGGCATGGACTGTGGTCAT-3'. The relative gene expression was calculated using the $2^{-\Delta\Delta Cq}$ method (22).

Western blotting. Proteins from MDA-MB-231 and MCF7 cells were extracted using RIPA cell lysis buffer (Santa Cruz Biotechnology, Inc.), and protein concentration was determined using a BCA assay kit. Protein samples (30 μg/lane) were separated using 10% SDS-PAGE. Proteins were transferred onto a PVDF membrane and blocked for 60 min in 0.05% Tween-20 in TBS (TBST) with 5% dried skim milk at room temperature. Immunoblot analysis was performed by incubating with the appropriate primary antibodies at 4˚C for 12 h. The membranes were then washed three times with TBST and incubated with a horseradish peroxidase-conjugated secondary antibody (1:20,000; cat. no. ab205718; Abcam) for 60 min at room temperature. Immunoreactive bands were visualized using an enhanced chemiluminescent detection kit (Beyotime Institute of Biotechnology). Signal quantification was obtained using Quantity One software (version 4.6.6; Bio-Rad Laboratories, Inc.) and normalized to β-actin.

Migration and wound healing assays. Cell migration assays were performed using Transwell® chambers (8-μM pores; Corning, Inc.). RPMI-1640 supplemented with 10% FBS was added to the bottom chamber. Transfected MDA-MB-231 and MCF7 cells ($5x10^4$) in serum-free IMDM were added to the upper chamber of each well. After incubation at 37˚C for 24 h, cells that had adhered to the membrane were fixed using 4% paraformaldehyde at room temperature for 20 min and stained with 0.1% crystal violet dye for 20 min at room temperature. Cells that had migrated through the membrane were imaged in six randomly selected fields of view using an inverted light microscope (magnification, x200). For the wound healing assays, a confluent monolayer of cells was scratched using a 250-μl pipette tip. Cells were cultured in serum-free RPMI-1640 medium. The wounded cell monolayer was observed under a light microscope (magnification, x100; Olympus Corporation) and images were taken at 0 and 24 h following the infliction of wounds, which was a cell-free nick created using Culture-Inserts. Closure of wounds was measured using ImageJ software (version 1.48; National Institutes of Health). Wound closure rates were expressed as percentages of the wound area closed at 24 h relative to the initial area of the cell-free region at 0 h.

Statistical analysis. SPSS software version 22.0 (IBM Corp.) and GraphPad Prism 6 (GraphPad Software, Inc.) were used for statistical analysis of the data. All data were expressed as the mean ± SD. F test was first used to check whether the variances are equal for statistical comparison, and then an unpaired two-tailed Student's t-test with equal variance was used for comparisons between two groups. Kolmogorov-Smirnov test was used to determine the normality of the distribution of data in each group. One-way ANOVA was used for making comparisons among multiple groups followed by Tukey's post-hoc test to assess the difference between 2 groups. $P<0.05$ was considered to indicate a statistically significant difference.

Results

miR150 serves a crucial role in gene regulation and patient prognosis. Through miRNA-mRNA co-expression network analysis, 19 miRNAs with >100 nodes were identified in the top 10,000 interactions (Fig. S1 and Table SI). According to the network properties, the miRNAs with the most nodes had the largest number of regulated genes; in this network, miR150 had the most nodes (Fig. 1A). Therefore, from the perspective of the co-expression network, miR150 had the most regulated genes compared with the other miRNAs. Lower expression levels of miR150 were observed in tumor samples compared with in adjacent samples at each stage (Fig. 1B). However, miR150 expression did not reach the criteria of a differentially expressed gene ($\log_2FC\geq|1|$ and $FDR\leq0.05$) in stages I-III (Fig. 1B). Additionally, Pearson's correlation analysis revealed that miR150 expression was negatively correlated with disease stage ($r=-0.13$; $P<0.001$; data not shown). Furthermore, 56 miRNAs were found to affect patient OS, while 25 miRNAs affected patient DFS (Tables SII and SIII). Among the top 20 miRNAs that were significantly associated with OS or DFS, low miR150 expression significantly decreased patient OS (Fig. 1C) and DFS (Fig. 1D). Based on the aforementioned results, it was hypothesized that miR150 served a vital role in breast cancer; thus, subsequent analyses focused on miR150.

miR150 target gene prediction. There were 9,583, 511, 8,436, 5,574 and 658 unique predicted miR150 target genes in microRNA, miRTarBase, mmmRNA, miRGate and miRDB, respectively (Fig. 2A and Table SIV). A total of 31 commonly predicted miR150 target genes were used for subsequent analyses. Among the 31 common target genes, BTLA exhibited the most positive significant correlation with miR150 (Fig. 2B). Furthermore, EGR2, EREG, LTBP2 and SGTB were positively correlated with miR150, while MYB and QSOX1 were negatively correlated with miR150. The correlation of BTLA, EGR2, EREG, LTBP2 and MYB expression with miR150 expression was validated in the GSE22220 dataset (Fig. S2); however, there was no data on SGTB or QSOX1 expression in this dataset. Since miR150 was not differentially expressed in the averaged whole tumor samples compared with the averaged adjacent samples, the specific paired expression differences of miR150 and its target genes in each tumor sample was compared with the mean expression of adjacent samples (calculated as the $\log_2$-transformed expression value of each tumor sample minus the mean $\log_2$-transformed value of all adjacent samples). Although miR150 did not reach significance in the entire cohort compared with the control group, ~two-thirds of patients exhibited low miR150 expression, whereas the remaining one-third of patients exhibited high miR150 expression compared with the controls. This suggested that the overall mean expression may mask some important information, and thus a more accurate personalized analysis method is required to reveal details that may otherwise be missed. Based on the individual expression differences, the mean expression value in the control group was used as the cut-off value for miR150. Accordingly, patients with miR150 ≥9.55 were defined as the high-miR150 group and those with miR150 <9.55 were defined as the low-miR150 group. In the follow-up analysis, the effects of high/low miR150 expression on global gene expression, pathway impairment and patient prognosis are described (Fig. 2C).

Low miR150 expression results in pathway impairment and gene deregulation. Multiple cancer-associated and immune-associated signaling pathways were upregulated in the low-miR150 group (such as 'pathways in cancer', 'B cell receptor signaling pathway', 'MAPK signaling pathway' and 'mTOR signaling pathway'), whereas only a few pathways were affected in the high-miR150 group (Fig. 3A and Table SV). Low miR150 expression was associated with multiple upregulated pathways also in the GSE22220 dataset (Fig. S3). There were 4,341 dysregulated genes in the high-miR150 vs. control groups, 4,374 dysregulated genes in the low-miR150 vs. control groups, and 717 dysregulated genes in the low-vs. high-miR150 groups (Fig. 3B and Tables SVI-SVIII). The 1,161 commonly upregulated genes and 2,357 downregulated genes between high-miR150 vs. controls and low-miR150 vs. controls were extracted (Fig. 3C), and the degree of $\log_2FC$ of these commonly dysregulated genes between high- and low-miR150 groups were compared (Fig. 3D and E). The results suggested that the effect on the commonly upregulated genes was similar between high- and low-miR150 groups; however, there were a greater

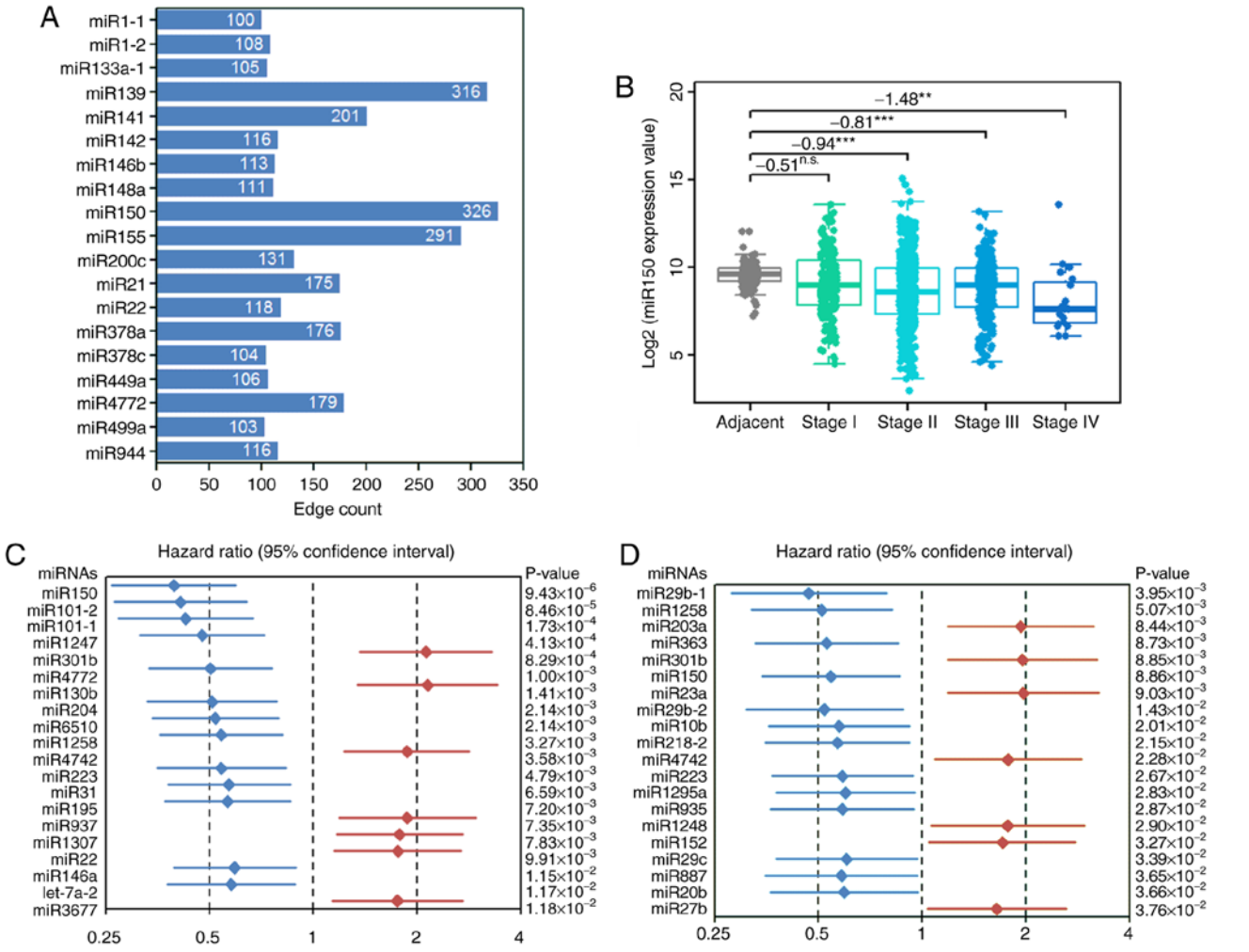

Figure 1. Bioinformatics analysis predicted miR150 to serve a crucial role in breast cancer. (A) Filtered miRNAs with edge counts >100 in the miRNA-mRNA co-expression network. Among the 19 filtered miRNAs, miR150 exhibited the maximum edge count. (B) miR150 expression in tumor and adjacent normal tissue samples stratified by stage. A one-way ANOVA with a post-hoc Tukey's test was used to compare the differences in miR150 expression between adjacent tissues and each tumor stage. The numbers indicate the $\log_2$(fold-change) between tumor and adjacent tissues. **P≤0.01; ***P≤0.001; n.s., no significance. (C) Effect of miRNAs on overall survival. (D) Effect of miRNAs on disease-free survival. Top 20 miRNAs according to significance. Diamonds represent the hazard ratio and the lines represent the 95% confidence interval. Red indicates high miRNA expression resulting in a worse prognosis and blue indicates high miRNA expression predictive of improved survival times. miRNA/miR, microRNA.

number of stronger influences of the commonly downregulated genes in low-vs. high-miR150 (mean logFCs of commonly upregulated and downregulated genes in low- vs. high-miR150 were: -0.045 and -0.270, respectively). These results suggested that low miR150 expression may result in a higher degree of downregulation of the targeted genes.

Overall analysis of the effects of miR150 on clinicopathological features and patient prognosis. Compared with patients with high-miR150, patients with low-miR150 were more likely to have a higher age at diagnosis and be ER$^+$, PR$^+$ and possess copy number alterations (Table I). Furthermore, miR150 was negatively associated with age at diagnosis, ER status, PR status, copy number alterations and stage (Table II). Using a univariate Cox regression model to assess the effect of miR150 and other clinical variables on patient prognosis, it was revealed that high miR150 expression was a protective factor of patient OS, but did not appear to affect DFS (Tables III and IV). Additionally, patients with positive ER or PR status exhibited improved OS and DFS compared with patients with a negative ER or PR status. Other factors, such as copy number alterations, number of lymph nodes examined, mutation count and stage also affected patient survival status. Therefore, a multivariate Cox regression model was used to analyze the independent effect of miR150 on patient prognosis with adjusted potential covariates (Table V). The results suggested that high miR150 expression independently predicted an improved patient OS.

Subgroup analysis of miR150 on patient prognosis. Considering the effects of hormonal receptor status and disease stage on patient prognosis, the independent effects of miR150 on patient OS and DFS in each subgroup were analyzed (Tables SIX-SXII). The prognostic analysis revealed that high miR150 expression significantly promoted patient OS in several subgroups (particularly in the ER$^-$ group); however, it had a relatively weak impact on patient DFS in different PR or HER groups, whereas it was significantly associated with patient DFS in the ER$^-$ group. Furthermore, high miR150 expression significantly improved patient OS in

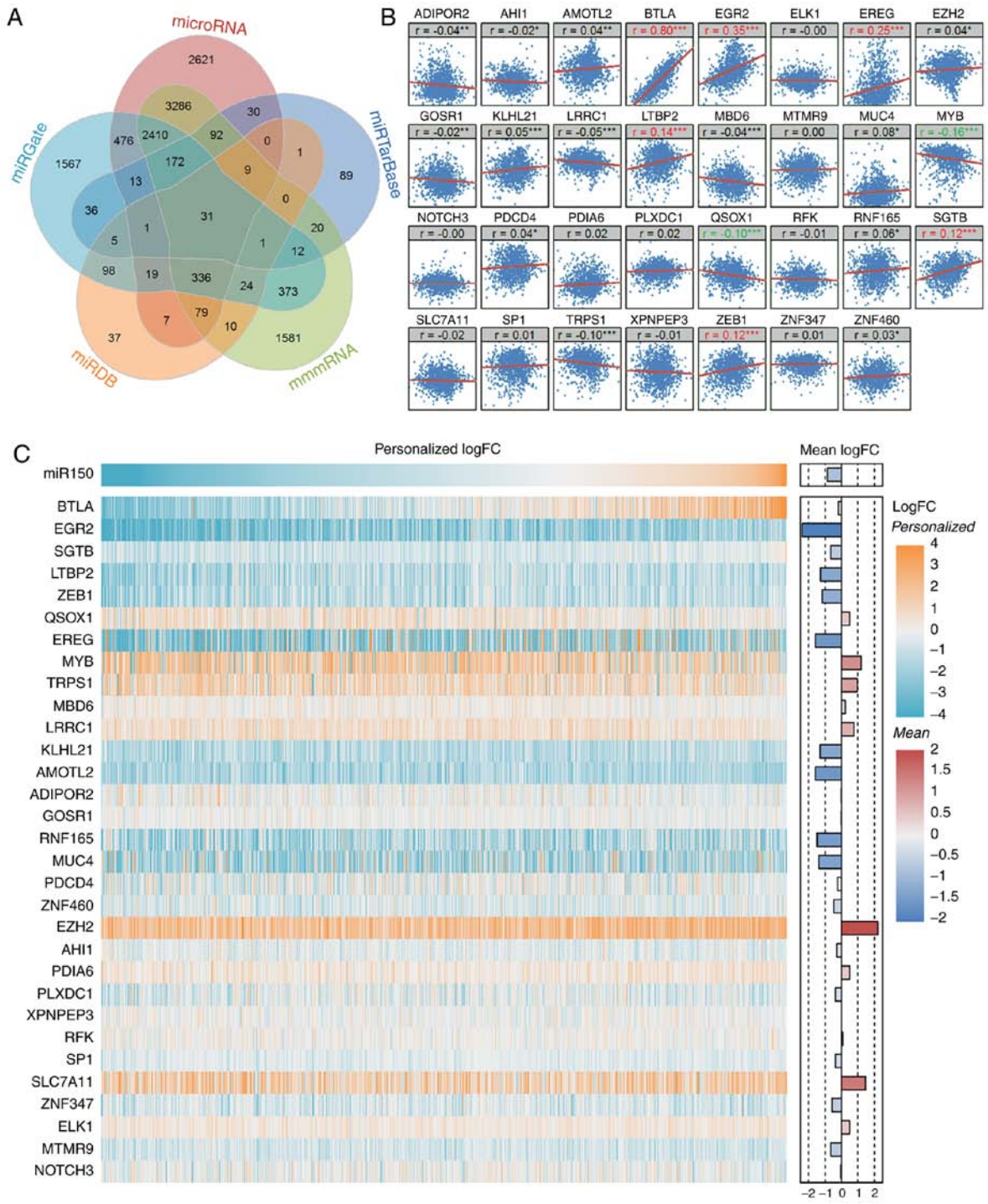

Figure 2. miR150 target gene prediction and expression. (A) Venn diagram of predicted miR150 targets based on 5 different web-based tools. (B) Linear correlation between miR150 and 31 commonly predicted miR150 target genes. The univariate linear model was used to calculate the correlation between miR150 and its target genes. Red indicates a gene was significantly positively correlated with miR150 and green indicates a gene was significantly negatively correlated with miR150. (C) Expression profiles of miR150 and its target genes. The personalized logFC was calculated as the $\log_2$-transformed expression value of each tumor sample minus the mean $\log_2$-transformed value of all adjacent samples. The mean logFC was calculated as the mean $\log_2$-transformed value of all tumor samples minus the mean $\log_2$-transformed value of all adjacent samples. The heatmap presents the personalized logFC of miR150 and target genes in patients. The red and blue bars represent the mean logFC of miR150 and target genes in patients. All target genes were sorted in descending order based on the Pearson correlation P-values. *P≤0.05; **P≤0.01; ***P≤0.001. FC, fold-change; miR, microRNA.

stage I/II groups and improved patient DFS in stage III/IV groups (Table SXII).

In the subgroup analysis grouped by median miR150 expression, the results revealed that low miR150 expression significantly decreased patient OS and DFS in the low-miR150 group, but not in the high-miR150 group (Fig. 4A-D). Since there was no information on hormone receptor status in the validation set, the overall impact of miR150 on patient prognosis was analyzed. The results revealed that low miR150 expression significantly decreased patient DFS, but did not significantly affect patient OS in the whole group or in the subgroups in the validation datasets (Fig. S4). Therefore, the

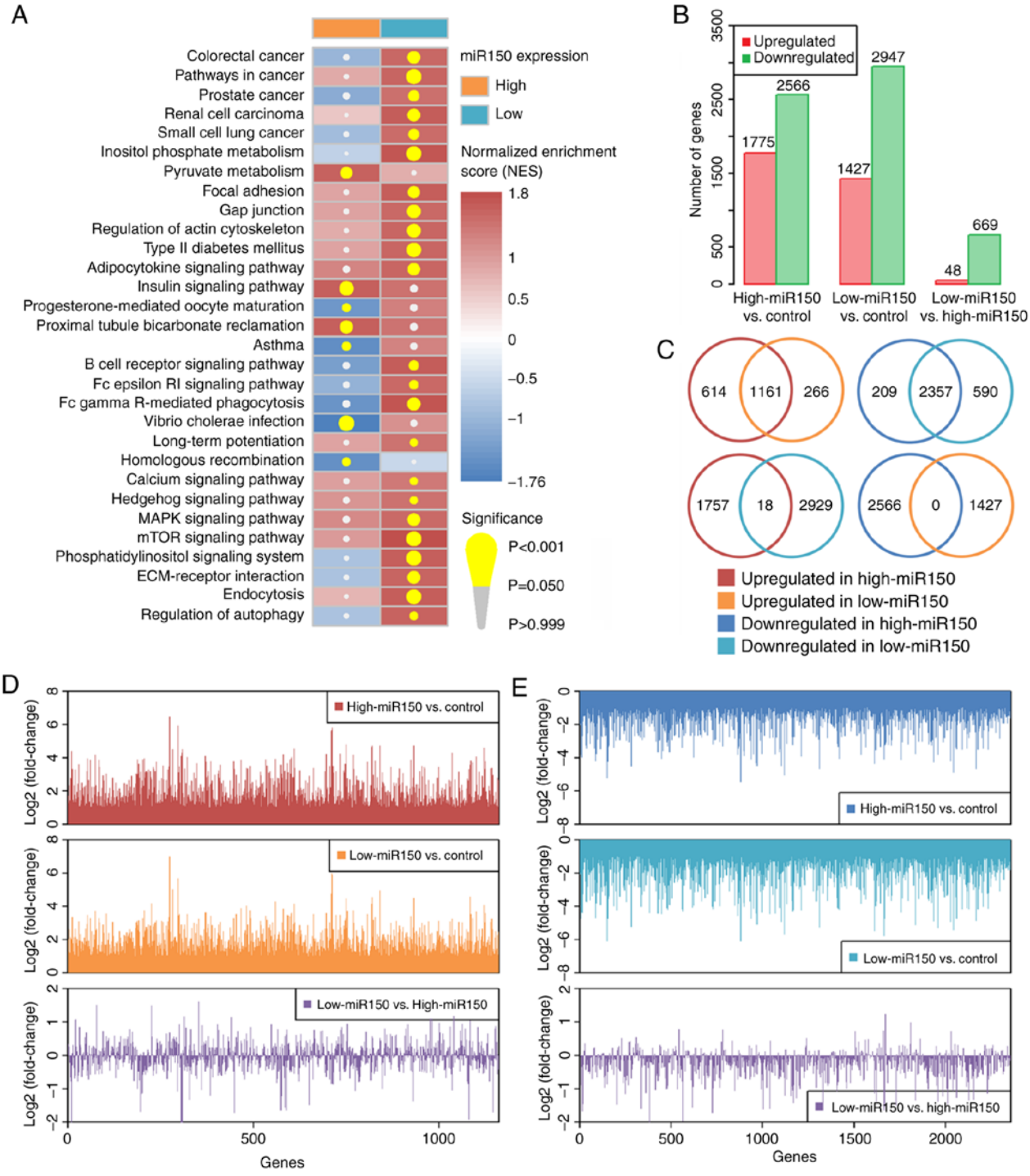

Figure 3. Effect of miR150 on KEGG pathways and global gene expression. (A) GSEA results of affected pathways in low- and high-miR150 groups. Significantly enriched KEGG pathways in each group are listed. (B) Number of dysregulated genes in low-miR150 vs. controls, high-miR150 vs. controls, and low-miR150 vs. high-miR150. (C) Venn diagrams of dysregulated genes in different groups. (D) Comparison of commonly upregulated genes between low- and high-miR150 groups. (E) Comparison of commonly downregulated genes between the low- and high-miR150 groups. The red and orange lines represent the log_2FC of commonly upregulated genes in high-miR150 vs. controls and low-miR150 vs. controls. The blue and cyan lines represent the log_2FC of commonly downregulated genes in high-miR150 vs. controls and low-miR150 vs. controls. The purple lines represent the log_2FC of the corresponding commonly dysregulated genes in low-vs. high-miR150. KEGG, Kyoto Encyclopedia of Genes and Genomes; miR, microRNA; GSEA, gene set enrichment analysis; FC, fold-change.

role of miR150 on the prognosis in patients with breast cancer requires further investigation.

Effect of miR150 target genes on patient prognosis. The effect of the 31 common miR150 target genes on patient OS (Fig. 4E) and DFS (Fig. 4F) were determined. The results revealed that BTLA and PDCD4 both positively affected patient OS and DFS. EGR2 and KLHL21 positively affected patient OS, XPNPEP3 negatively affected patient OS, NOTCH3 negatively affected patient DFS and RNF165 positively affected patient DFS. In the interaction analysis of miR150 and its target genes on patient prognosis, miR150 and

Table I. Clinicopathological features of patients with breast invasive carcinoma grouped by microRNA 150 expression.

Variable	Low expression	High expression	P-value
Age at diagnosis[a], years	59.7±13.4	56.1±12.5	<0.001[b]
Ethnicity, n (%)			0.037[c]
White	502 (77.6)	240 (70.8)	
Asian	39 (6.0)	22 (6.5)	
African American	106 (16.4)	76 (22.4)	
American Indian or Alaska Native	0 (0.0)	1 (0.3)	
Estrogen receptor status, n (%)			<0.001[b]
Negative	119 (17.2)	113 (34.0)	
Positive	574 (82.8)	219 (66.0)	
Progesterone receptor status, n (%)			<0.001[b]
Negative	198 (28.7)	137 (41.3)	
Positive	492 (71.3)	195 (58.7)	
Human epidermal growth factor receptor 2 status, n (%)			0.608
Negative	228 (80.6)	100 (83.3)	
Positive	55 (19.4)	20 (16.7)	
Copy number alterations[a]	0.30±0.2	0.27±0.2	0.044[c]
Lymph nodes examined number[a]	10.6±8.5	10.6±9.3	0.964
Mutation count[a]	66.0±239.9	57.5±135.5	0.482
Stage, n (%)			0.378
I	113 (16.0)	67 (19.3)	
II	410 (58.2)	198 (56.9)	
III	166 (23.5)	79 (22.7)	
IV	16 (2.3)	4 (1.1)	

[a]Mean ± SEM; [b]P<0.001; [c]P<0.05. Low expression, <9.55; high expression, ≥9.55.

Table II. Univariate linear regression analysis of microRNA 150 expression and clinicopathological features.

Variable	N[a]	Mean ± SD	β (SE)	P-value
Age at diagnosis	1,074		-0.02 (0.00)	<0.001[b]
Estrogen receptor status				
Negative	232	9.29±2.05	Reference	
Positive	793	8.52±1.73	-0.77 (0.13)	<0.001[b]
Progesterone receptor status				
Negative	335	8.95±2.00	Reference	
Positive	687	8.56±1.73	-0.39 (0.12)	0.002[c]
Human epidermal growth factor receptor 2 status				
Negative	328	8.63±1.83	Reference	
Positive	75	8.41±1.78	-0.22 (0.23)	0.356
Copy number alterations	1,059		-1.21 (0.27)	<0.001[b]
Lymph nodes examined number	954		0.01 (0.01)	0.420
Mutation count	957		-0.00 (0.00)	0.730
Stage				
Stage I	180	9.04±1.84	Reference	
Stage II	608	8.62±1.89	-0.42 (0.16)	0.008[c]
Stage III	245	8.75±1.67	-0.15 (0.09)	0.087
Stage IV	20	8.08±1.79	-0.32 (0.14)	0.027

[a]Number of samples (some of these variables have missing values); [b]P<0.001; [c]P<0.01. SE, standard error.

Table III. Univariate Cox regression analysis of miR150 expression, clinicopathological features and overall survival.

Variable	N[a]	Median (Q1-Q3), months	HR (95% CI)	P-value
miR150 (continuous)	1,073		0.89 (0.82-0.97)	0.010[b]
miR150 (categorical)[c]				
Low expression	718	23.90 (13.68-50.33)	Reference	
High expression	355	36.10 (18.35-70.91)	0.63 (0.44-0.90)	0.012[b]
Age at diagnosis	1,073		1.03 (1.02-1.04)	<0.001[d]
Estrogen receptor status				
Negative	232	29.88 (13.49-58.59)	Reference	
Positive	793	26.97 (15.60-55.45)	0.68 (0.47-0.99)	0.042[b]
Progesterone receptor status				
Negative	335	27.99 (13.59-56.73)	Reference	
Positive	687	27.56 (16.21-55.42)	0.72 (0.51-1.02)	0.065
Human epidermal growth factor receptor 2 status				
Negative	328	33.10 (18.50-62.02)	Reference	
Positive	75	32.72 (15.46-55.42)	0.89 (0.40-2.00)	0.779
Copy number alterations	1,056		2.65 (1.27-5.55)	0.009[e]
Lymph nodes examined number	953		1.02 (1.00-1.04)	0.060
Mutation count[f]	956		1.00 (1.00-1.00)	0.001[e]
Stage				
Stage I	180	39.52 (20.74-72.49)	Reference	
Stage II	607	26.02 (14.75-53.47)	1.72 (0.98-3.02)	0.060
Stage III	245	23.23 (13.07-46.62)	3.17 (1.76-5.69)	<0.001[d]
Stage IV	20	26.56 (9.59-39.59)	14.18 (6.69-30.04)	<0.001[d]

[a]Number of samples (some of these variables have missing values); [b]P<0.05; [c]low, miR150 <9.55 and high, miR150 ≥9.55; [d]P<0.001; [e]P<0.01; [f]The more accurate HR (95% CI) in the mutation count is 1.001 (1.001-1.002). HR, hazard ratio; CI, confidence interval; miR150, microRNA 150.

7 genes (BTLA, EGR2, NOTCH3, PDIA6, QSOX1, SLC7A11 and ZNF460) interactively affected both patient OS and DFS (Table SXIII).

miR150 affects cell viability and migratory capacity of breast cancer cells. MDA-MB-231 cells were transfected with the miR150 mimics and MCF7 cells were transfected with the miR150 inhibitors; the transfection efficiency is shown in Fig. 5A. To explore the effects of miR150 on migration and viability of breast cancer cells, miR150 was overexpressed in MDA-MB-231 cells via transfection of the miR150 mimics using a mimics NC as the control, while MCF7 cells were transfected with the designed inhibitors to decrease miR150 expression levels. The results indicated that cell viability was significantly decreased in the miR150 overexpression group compared with in the control group (Fig. 5B). Compared with in the inhibitors NC group, MCF7 cell viability was significantly increased in the miR150 inhibitor group (Fig. 5B), suggesting that overexpression of miR150 decreased the viability of breast cancer cells. Transwell® assays revealed that overexpression of miR150 significantly decreased cell migration (Fig. 5C), whereas inhibition of miR150 significantly increased cell migration (Fig. 5D). These results were further confirmed by wound healing assays, which demonstrated that cell mobility was significantly decreased in the overexpressed miR150 group (Fig. 5E), while it was significantly increased in the miR150 inhibited group (Fig. 5F). Overall, these results indicated that miR150 decreased breast cancer cell viability and migration.

Subsequently, the effect of the interaction between miR150 and BTLA on breast cancer cell migration was analyzed. The mRNA and protein expression levels of BTLA were significantly increased when miR150 was overexpressed (Figs. 5G, H and S5A), while they were significantly decreased when miR150 expression was knocked down (Figs. 5G, I and S5B). To further test whether the migratory capacity of breast cancer cells was directly dependent on BTLA, a siRNA targeting BTLA (si-BTLA; Fig. S6) and a miR150 inhibitor were co-transfected to concurrently knock down BTLA and miR150 expression in MCF7 cells (Fig. 5J). Concurrent knockdown of BTLA and miR150 expression resulted in a considerably more severe phenotype than either miR150 inhibitors or si-BTLA alone (Fig. 5K and L). In summary, the present results demonstrated that miR150 may regulate cell migration by directly regulating BTLA expression.

Discussion

An increasing number of studies have shown that numerous miRNAs exhibit varying roles in the pathophysiology of breast cancer, such as facilitating invasion and metastasis, inducing epithelial-mesenchymal transition and maintaining breast cancer stem cell proliferation. miRNAs regulate gene

Table IV. Univariate Cox regression analysis of miR150 expression, clinicopathological features and disease-free survival.

Variable	N[a]	Median (Q1-Q3), months	HR (95% CI)	P-value
miR150 (continuous)	984		0.91 (0.83-1.01)	0.068
miR150 (categorical)[b]				
Low expression	651	21.91 (13.01-42.79)	Reference	
High expression	333	33.67 (17.12-68.69)	0.70 (0.47-1.05)	0.083
Age at diagnosis	984		1.01 (0.99-1.02)	0.485
Estrogen receptor status				
Negative	215	24.97 (12.68-53.38)	Reference	
Positive	727	24.70 (14.87-50.77)	0.56 (0.37-0.83)	0.004[c]
Progesterone receptor status				
Negative	310	23.25 (12.92-53.15)	Reference	
Positive	628	24.98 (15.31-49.92)	0.54 (0.37-0.80)	0.002[c]
Human epidermal growth factor receptor 2 status				
Negative	310	31.70 (17.81-59.24)	Reference	
Positive	69	32.72 (14.68-55.45)	0.47 (0.17-1.32)	0.153
Copy number alterations	968		1.80 (0.74-4.40)	0.196
Lymph nodes examined number	878		1.02 (1.00-1.04)	0.031[d]
Mutation count[e]	875		1.00 (1.00-1.00)	0.920
Stage				
Stage I	168	37.55 (20.02-63.90)	Reference	
Stage II	565	23.52 (13.96-48.19)	1.66 (0.86-3.20)	0.132
Stage III	224	21.73 (12.44-42.91)	3.73 (1.91-7.32)	<0.001[f]
Stage IV	10	23.24 (8.46-44.40)	13.98 (4.95-39.50)	<0.001[f]

[a]Number of samples (some of these variables have missing values); [b]low, miR150 <9.55 and high, miR150 ≥9.55; [c]P<0.01; [d]P<0.05; [e]the more accurate HR (95% CI) in the mutation count is 1.001 (0.997-1.002); [f]P<0.001. HR, hazard ratio; CI, confidence interval; miR150, microRNA 150.

expression at numerous levels, including epigenetic and genetic alterations, and transcriptional repression (3-9). Several studies have demonstrated that each miRNA is capable of regulating the expression of multiple downstream genes (5-7); therefore, one miRNA can simultaneously regulate multiple cellular signaling pathways (4). The present study revealed that miR150 and its potential target genes (including BTLA, EGR2, EREG, MYB and LTPB2) resulted in the upregulation of several carcinogenic and signaling transduction pathways, ultimately leading to breast cancer development and/or progression. Additionally, downregulation of miR150 expression decreased OS in patients with breast cancer. Functional *in vitro* experiments demonstrated that a miR150-BTLA axis regulated cell migration.

Previous studies revealed that aberrant activation of these miR150-associated signaling transduction pathways (such as the Wnt/β-catenin and Notch signaling pathways) accelerated breast cancer progression (23-25). In human breast cancer cell lines, the Wnt/β-catenin signaling pathway activates Lin28 expression and represses let-7 expression, leading to expansion of breast cancer stem cells (23). The Notch signaling pathway is required for stem cell maintenance in breast cancer (24). Through directly targeting NOTCH1, it was revealed that ectopic miR34a expression decreases cancer stem cell properties and increases their sensitivity to doxorubicin treatment (25). Furthermore, increased miR34 expression results in cell cycle arrest, whereas its downregulation increases the invasive capacity and metastatic potential of breast cancer cell lines (25). The present study demonstrated that low miR150 expression may activate these signaling transduction pathways. Considering the carcinogenic effects of these pathways in breast cancer, it was speculated that increasing the expression levels of miR150 may facilitate breast cancer treatment and prolong patient survival.

The antitumor effects of miR150 have been demonstrated in several types of cancer. Li *et al* (26) revealed that upregulated miR150 expression suppresses proliferation and tumorigenicity via targeting multiple cell cycle-associated genes (including CCND1, CCND2, CDK2 and CCNE2) in nasopharyngeal carcinoma *in vitro* and *in vivo*. In non-small cell lung cancer cell lines, suppression of miR150 inhibits proliferation by inactivating the AKT and the SIRT2/JMJD2A signaling pathways (27). Furthermore, downregulated miR150 expression decreases the inhibition of HIG2 and promotes proliferation, motility, apoptosis and iron metabolism in hepatocellular carcinoma cell lines (28). The present study demonstrated that in patients with low expression levels of miR150 who were ER^+ and PR^+, dysregulation of signaling pathways was more severe, resulting in less favorable outcomes. A recent triple-negative breast cancer study revealed that miR150 expression is downregulated in tumor tissues compared with in normal breast tissues, and that ectopic

Table V. Multivariate Cox regression analysis of miR150 expression and patient survival.

A, Overall survival

Variable	N[a]	Median (Q1-Q3), months	HR (95% CI)	P-value[b]
miR150 (continuous)	1,073		0.71 (0.58-0.87)	0.001[c]
miR150 (categorical)[d]				
Low expression	718	23.90 (13.68-50.33)	Reference	
High expression	355	36.10 (18.35-70.91)	0.31 (0.12-0.78)	0.013[e]

B, Disease-free survival

Variable	N[a]	Median (Q1-Q3), months	HR (95% CI)	P-value[b]
miR150 (continuous)	984		0.78 (0.63-0.95)	0.015[e]
miR150 (categorical)[d]				
Low expression	651	21.91 (13.01-42.79)	Reference	
High expression	333	33.67 (17.12-68.69)	0.54 (0.24-1.24)	0.146

[a]Number of samples (some of these variables have missing values); [b]P-values were adjusted for diagnosis age, estrogen receptor status, progesterone receptor status, human epidermal growth factor receptor 2 status, copy number alterations, lymph nodes examined number, mutation count and stage; [c]P<0.01; [d]Low, miR150 <9.55 and high, miR150 ≥9.55; [e]P<0.05. HR, hazard ratio; CI, confidence interval; miR150, microRNA 150.

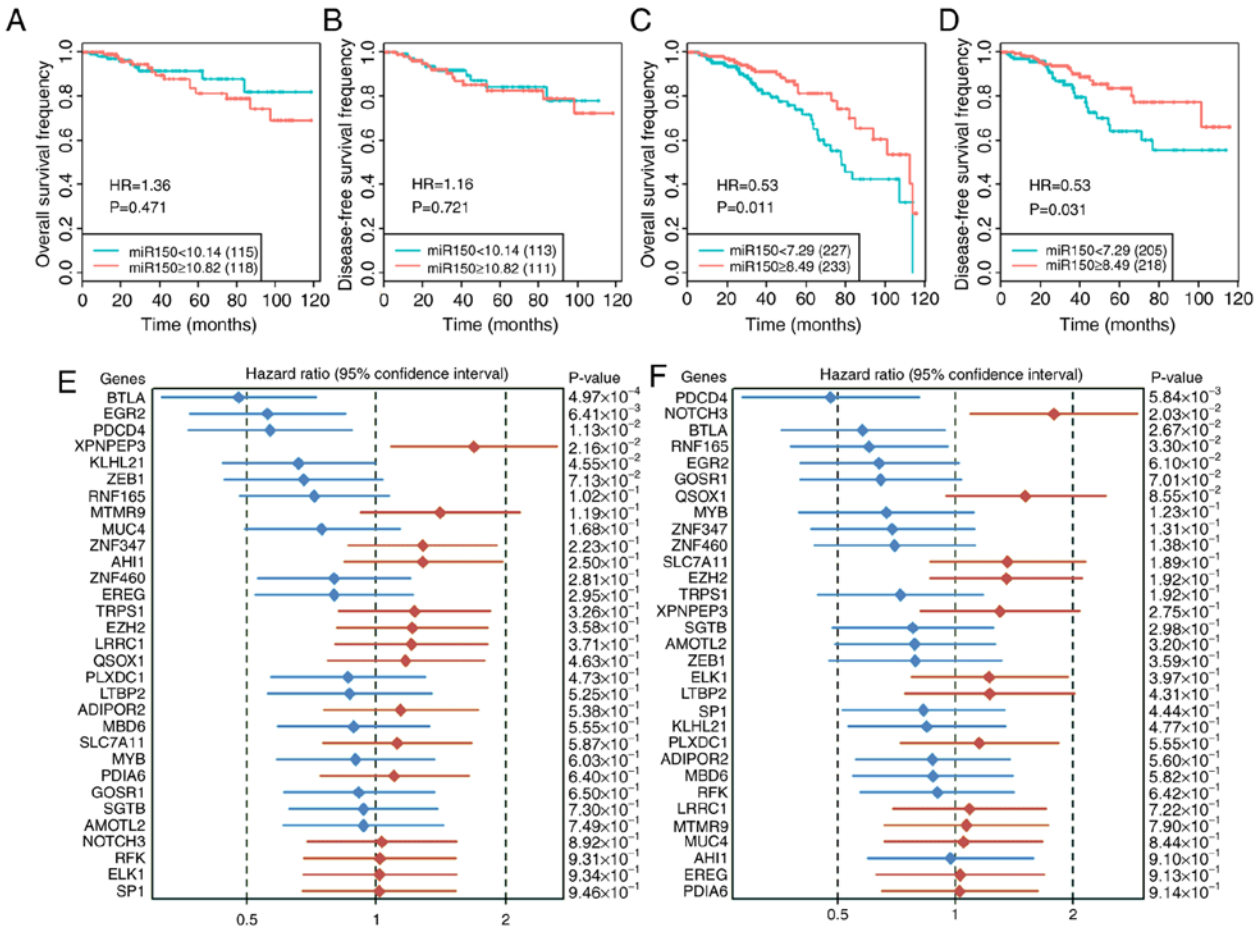

Figure 4. Effect of miR150 and its target genes on patient prognosis. Effect of miR150 on patient (A) overall and (B) disease-free survival in the high-miR150 group. Effect of miR150 on (C) overall and (D) disease-free survival in the low-miR150 group. Effect of miR150 target genes on patient (E) overall and (F) disease-free survival. The diamonds represent the hazard ratio and the lines represent the 95% confidence interval. Red indicates high miRNA expression and a worse prognosis, and blue indicates high mRNA expression and prolonged survival time. miR, microRNA; HR, hazard ratio.

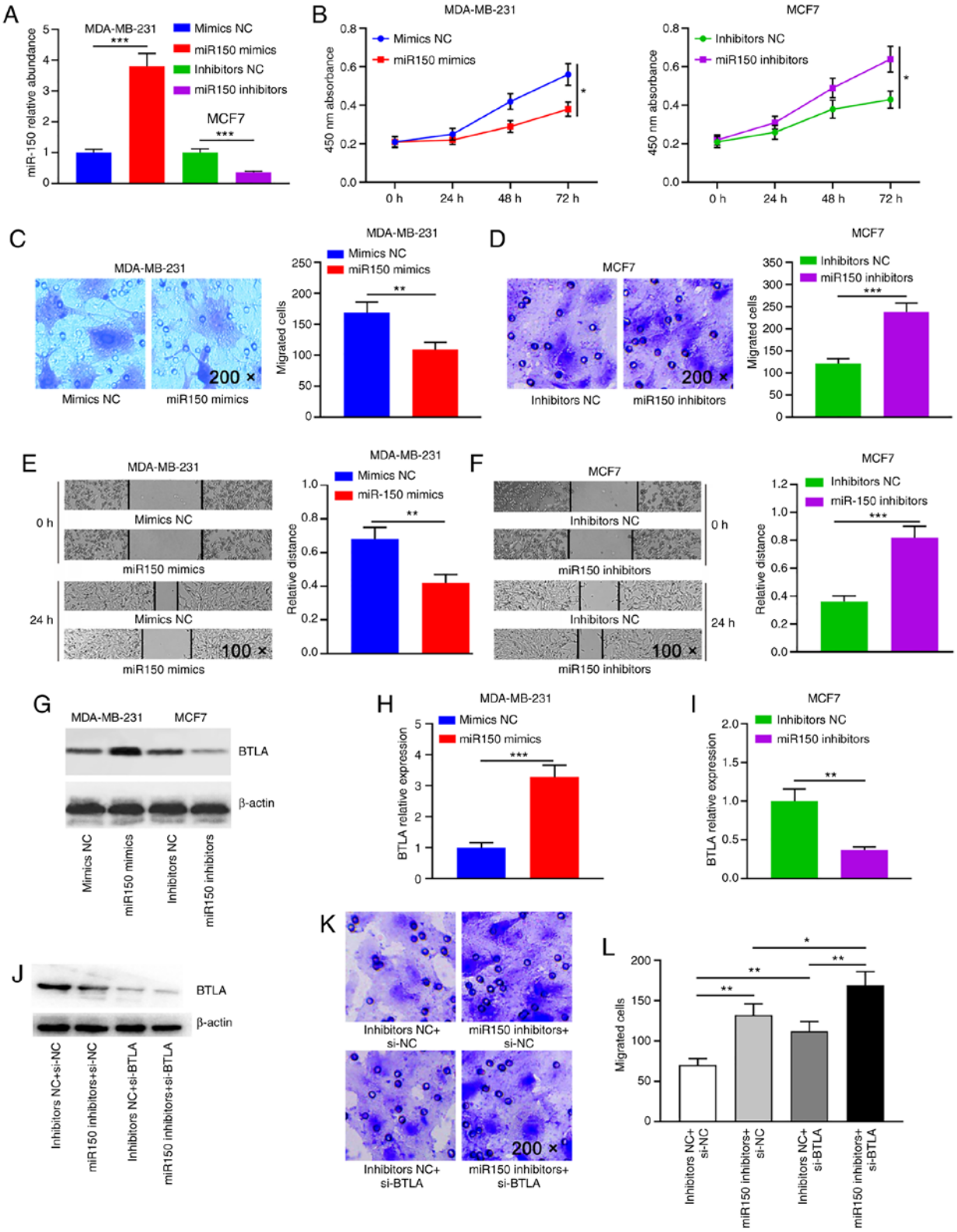

Figure 5. miR150 inhibits breast cancer cell viability and migration via BTLA. (A) Reverse transcription-quantitative PCR was used to detect miR150 expression in MDA-MB-231 and MCF7 cells transfected with miR150 mimics/inhibitors. miR150 RNA levels are expressed as the mean ± SD of four different experiments normalized to U6. (B) CCK-8 assay was performed to assess the effect of miR150 overexpression or knockdown on cell viability in MDA-MB-231 and MCF-7 cells, respectively. Representative microscopic images and cell counts of migratory cells from (C) the mimics-transfected MDA-MB-231 breast cancer cells and (D) the inhibitors-transfected MCF7 breast cancer cells in a Transwell® assay (magnification, x200). Representative microscopic images of wound healing in (E) the miR150-overexpressing MDA-MB-231 cells and (F) the miR150-knockdown MCF7 cells (magnification, x100). Data from the CCK-8 cell viability, Transwell® migration and wound healing assays are presented as the mean ± SEM of three independent repeats. (G) Western blot of BTLA expression in the different miR150-treated groups. Densitometry analysis was performed to assess expression in (H) MDA-MB-231 and (I) MCF7 cells. BTLA protein expression levels are expressed as the mean ± SEM of three different experiments normalized to β-actin levels. (J) Western blot of BTLA expression in different treatment groups. (K) Transwell® assays were performed to detect the migratory capacity of treated cells (magnification, x200). (L) Quantification of the Transwell® assays. *P≤0.05; **P≤0.01; ***P≤0.001. miR, microRNA; BTLA, B and T lymphocyte attenuator; NC, negative control; si, small interfering; CCK-8, Cell Counting Kit-8.

miR150 expression suppresses tumor cell migration and metastasis (29). Monocytes are important for tumor immunity. Shu *et al* (30) demonstrated that miR150-5p suppresses CCR2 expression by targeting Notch 3 in breast cancer monocytes, thus inhibiting tumorigenesis. However, a previous study revealed that miR150 expression was upregulated in tumor tissues and breast cancer cell lines, suggesting that high miR150 expression is associated with increased cell proliferation (31). The aforementioned studies are all focused on the entire cohorts used in each study, which may ignore the differences between individuals. In the present study, miR150 was not dysregulated in the entire cohort; however, in the subgroup analysis, there was a significant difference in patients with low levels of miR150 compared with those expressing high levels. Therefore, increased stratification and personalized research may assist in identifying and understanding the biological mechanisms of cancer.

There were 8 genes (BTLA, EGR2, EREG, LTBP2, SGTB, MYB, ZEB1 and QSOX1) that were significantly correlated with miR150 among the 31 predicted miR150 target genes in the present study. Several studies have identified EGR2 as a target of miR150; upregulated miR150 regulates EGR2-promoted gastric cancer cell proliferation (32) and the development of chronic rhinosinusitis (33). A previous study revealed that there were four miR150 binding sites in the 3'-untranslated region of c-Myb, and found that miR150 decreased endogenous c-Myb mRNA and protein expression levels by half (34). A recent study demonstrated that upregulation of miR150 significantly inhibits the proliferation, migration and invasion of melanoma cells by suppressing MYB (35). Furthermore, decreased miR150 expression results in increased c-Myb expression in B-lymphocytes in patients with autoimmune hemolytic anemia/Evans syndrome (36). BTLA is a member of the immunoglobulin superfamily and functions in immune response inhibition (37,38). Gene polymorphisms of BTLA were associated with an increased risk of sporadic breast cancer and a less favorable prognosis (37). By lowering BTLA levels using neutralizing antibodies, downregulation of BTLA decreases anti-tumor immunity in natural killer T cells (38). The results of the present study revealed that miR150 positively regulated BTLA expression, and concurrent downregulation of miR150 and BTLA promoted cell migration.

In conclusion, the present study indicated that low miR150 expression was associated with less favorable clinicopathological characteristics, upregulation of multiple carcinogenic pathways and poor patient survival. miR150 expression was significantly negatively correlated with disease stage, and may thus be used as a marker of advanced stage breast cancer. Through miRNA target gene prediction and correlation analysis, BTLA, EGR2 and MYB were significantly correlated with miR150 expression in both the TCGA-BRCA and validation datasets. The strong positive association between miR150 and BTLA was verified by functional *in vitro* experiments. Furthermore, experimental results suggested that miR150 and BTLA promoted cell migration. Therefore, the present study suggested that increasing miR150 expression or interfering with its target genes may serve as a potential form of breast cancer treatment aimed at improving patient survival.

Acknowledgements

Not applicable.

Funding

The present study was supported by grants from the National Natural Science Foundation of China (grant nos. 81071990 and 81641110), the Natural Science Foundation Guangdong Province (grant no. 2015A030313725), the Science and Technology Program of Guangzhou (grant no. 201707010305), the Medical Research Foundation of Guangdong Province (grant no. A2017427) and the Youth Science Foundation of Guangdong Second Provincial General Hospital (grant no. YQ2016-001).

Availability of data and materials

The datasets generated and/or analyzed during the current study are available in The Cancer Genome Atlas database (cancergenome.nih.gov/) for the TCGA-BRCA dataset and in Gene Expression Omnibus database (ncbi.nlm.nih.gov/geo/) for the microarray datasets GSE22216, GSE22219, GSE22220 and GSE40267.

Authors' contributions

SQA, KH, GAX and WXL designed the study. SQA, KH, FL, QSD and WXL collected the data. SQA, KH, YLW, ZLX, XPD, RH and WXL performed the data analysis and visualization. KH, FL, QSD, BWL, HHW and YT performed the experiments. SQA, KH, BWL, HHW, GAX and WXL wrote the manuscript. SQA, KH, GAX and WXL revised the manuscript. All authors read and approved the final manuscript.

Ethics approval and consent to participate

Not applicable.

Patient consent for publication

Not applicable.

Competing interests

The authors declare that they have no competing interests.

References

1. Chen W, Zheng R, Baade PD, Zhang S, Zeng H, Bray F, Jemal A, Yu XQ and He J: Cancer statistics in China, 2015. CA Cancer J Clin 66: 115-132, 2016.
2. Giuliano AE, Connolly JL, Edge SB, Mittendorf EA, Rugo HS, Solin LJ, Weaver DL, Winchester DJ and Hortobagyi GN: Breast cancer-major changes in the American joint committee on cancer eighth edition cancer staging manual. CA Cancer J Clin 67: 290-303, 2017.
3. Bertoli G, Cava C and Castiglioni I: MicroRNAs: New biomarkers for diagnosis, prognosis, therapy prediction and therapeutic tools for breast cancer. Theranostics 5: 1122-1143, 2015.
4. Bartel DP: Metazoan MicroRNAs. Cell 173: 20-51, 2018.
5. Zhang ZJ and Ma SL: miRNAs in breast cancer tumorigenesis (Review). Oncol Rep 27: 903-910, 2012.

6. Aure MR, Leivonen SK, Fleischer T, Zhu Q, Overgaard J, Alsner J, Tramm T, Louhimo R, Alnaes GI, Perälä M, *et al*: Individual and combined effects of DNA methylation and copy number alterations on miRNA expression in breast tumors. Genome Biol 14: R126, 2013.
7. Ma L, Teruya-Feldstein J and Weinberg RA: Tumour invasion and metastasis initiated by microRNA-10b in breast cancer. Nature 449: 682-688, 2007.
8. Iorio MV, Ferracin M, Liu CG, Veronese A, Spizzo R, Sabbioni S, Magri E, Pedriali M, Fabbri M, Campiglio M, *et al*: MicroRNA gene expression deregulation in human breast cancer. Cancer Res 65: 7065-7070, 2005.
9. Blenkiron C, Goldstein LD, Thorne NP, Spiteri I, Chin SF, Dunning MJ, Barbosa-Morais NL, Teschendorff AE, Green AR, Ellis IO, *et al*: MicroRNA expression profiling of human breast cancer identifies new markers of tumor subtype. Genome Biol 8: R214, 2007.
10. He K, Li WX, Guan D, Gong M, Ye S, Fang Z, Huang JF and Lu A: Regulatory network reconstruction of five essential microRNAs for survival analysis in breast cancer by integrating miRNA and mRNA expression datasets. Funct Integr Genomics 19: 645-658, 2019.
11. Betel D, Wilson M, Gabow A, Marks DS and Sander C: The microRNA.org resource: Targets and expression. Nucleic Acids Res 36: D149-D153, 2008.
12. Chou CH, Shrestha S, Yang CD, Chang NW, Lin YL, Liao KW, Huang WC, Sun TH, Tu SJ, Lee WH, *et al*: miRTarBase update 2018: A resource for experimentally validated microRNA-target interactions. Nucleic Acids Res 46: D296-D302, 2018.
13. Tabas-Madrid D, Muniategui A, Sánchez-Caballero I, Martinez-Herrera DJ, Sorzano CO, Rubio A and Pascual-Montano A: Improving miRNA-mRNA interaction predictions. BMC Genomics 15 (Suppl 10): S2, 2014.
14. Andrés-León E, González Peña D, Gómez-López G and Pisano DG: miRGate: A curated database of human, mouse and rat miRNA-mRNA targets. Database (Oxford) 2015: bav035, 2015.
15. Wong N and Wang X: miRDB: An online resource for microRNA target prediction and functional annotations. Nucleic Acids Res 43: D146-D152, 2015.
16. Ekimler S and Sahin K: Computational methods for microRNA target prediction. Genes (Basel) 5: 671-683, 2014.
17. Buffa FM, Camps C, Winchester L, Snell CE, Gee HE, Sheldon H, Taylor M, Harris AL and Ragoussis J: microRNA-associated progression pathways and potential therapeutic targets identified by integrated mRNA and microRNA expression profiling in breast cancer. Cancer Res 71: 5635-5645, 2011.
18. de Rinaldis E, Gazinska P, Mera A, Modrusan Z, Fedorowicz GM, Burford B, Gillett C, Marra P, Grigoriadis A, Dornan D, *et al*: Integrated genomic analysis of triple-negative breast cancers reveals novel microRNAs associated with clinical and molecular phenotypes and sheds light on the pathways they control. BMC Genomics 14: 643, 2013.
19. Ritchie ME, Phipson B, Wu D, Hu Y, Law CW, Shi W and Smyth GK: limma powers differential expression analyses for RNA-sequencing and microarray studies. Nucleic Acids Res 43: e47, 2015.
20. Huynh-Thu VA, Irrthum A, Wehenkel L and Geurts P: Inferring regulatory networks from expression data using tree-based methods. PLoS One 5: e12776, 2010.
21. Subramanian A, Tamayo P, Mootha VK, Mukherjee S, Ebert BL, Gillette MA, Paulovich A, Pomeroy SL, Golub TR, Lander ES and Mesirov JP: Gene set enrichment analysis: A knowledge-based approach for interpreting genome-wide expression profiles. Proc Natl Acad Sci USA 102: 15545-15550, 2005.
22. Livak KJ and Schmittgen TD: Analysis of relative gene expression data using real-time quantitative PCR and the 2(-Delta Delta C(T)) method. Methods 25: 402-408, 2001.
23. Cai WY, Wei TZ, Luo QC, Wu QW, Liu QF, Yang M, Ye GD, Wu JF, Chen YY, Sun GB, *et al*: The wnt-β-catenin pathway represses let-7 microRNA expression through transactivation of lin28 to augment breast cancer stem cell expansion. J Cell Sci 126: 2877-2889, 2013.
24. Park EY, Chang E, Lee EJ, Lee HW, Kang HG, Chun KH, Woo YM, Kong HK, Ko JY, Suzuki H, *et al*: Targeting of miR34a-NOTCH1 axis reduced breast cancer stemness and chemoresistance. Cancer Res 74: 7573-7582, 2014.
25. Yang S, Li Y, Gao J, Zhang T, Li S, Luo A, Chen H, Ding F, Wang X and Liu Z: MicroRNA-34 suppresses breast cancer invasion and metastasis by directly targeting Fra-1. Oncogene 32: 4294-4303, 2013.
26. Li X, Liu F, Lin B, Luo H, Liu M, Wu J, Li C, Li R, Zhang X, Zhou K and Ren D: miR-150 inhibits proliferation and tumorigenicity via retarding G1/S phase transition in nasopharyngeal carcinoma. Int J Oncol 50: 1097-1108, 2017.
27. Jiang K, Shen M, Chen Y and Xu W: miR-150 promotes the proliferation and migration of nonsmall cell lung cancer cells by regulating the SIRT2/JMJD2A signaling pathway. Oncol Rep 40: 943-951, 2018.
28. Xu Y, Luo X, He W, Chen G, Li Y, Li W, Wang X, Lai Y and Ye Y: Long non-coding RNA PVT1/miR-150/ HIG2 axis regulates the proliferation, invasion and the balance of iron metabolism of hepatocellular carcinoma. Cell Physiol Biochem 49: 1403-1419, 2018.
29. Tang W, Xu P, Wang H, Niu Z, Zhu D, Lin Q, Tang L and Ren L: MicroRNA-150 suppresses triple-negative breast cancer metastasis through targeting HMGA2. Onco Targets Ther 11: 2319-2332, 2018.
30. Shu L, Wang Z, Wang Q, Wang Y and Zhang X: Signature miRNAs in peripheral blood monocytes of patients with gastric or breast cancers. Open Biol 8: 180051, 2018.
31. Huang S, Chen Y, Wu W, Ouyang N, Chen J, Li H, Liu X, Su F, Lin L and Yao Y: miR-150 promotes human breast cancer growth and malignant behavior by targeting the pro-apoptotic purinergic P2X7 receptor. PLoS One 8: e80707, 2013.
32. Wu Q, Jin H, Yang Z, Luo G, Lu Y, Li K, Ren G, Su T, Pan Y, Feng B, *et al*: MiR-150 promotes gastric cancer proliferation by negatively regulating the pro-apoptotic gene EGR2. Biochem Biophys Res Commun 392: 340-345, 2010.
33. Ma Z, Shen Y, Zeng Q, Liu J, Yang L, Fu R and Hu G: MiR-150-5p regulates EGR2 to promote the development of chronic rhinosinusitis via the DC-Th axis. Int Immunopharmacol 54: 188-197, 2018.
34. Barroga CF, Pham H and Kaushansky K: Thrombopoietin regulates c-myb expression by modulating micro RNA 150 expression. Exp Hematol 36: 1585-1592, 2008.
35. Sun X, Zhang C, Cao Y and Liu E: miR-150 suppresses tumor growth in melanoma through downregulation of MYB. Oncol Res 21: 317-323, 2019.
36. Xing L, Xu W, Qu Y, Zhao M, Zhu H, Liu H, Wang H, Su X and Shao Z: miR-150 regulates B lymphocyte in autoimmune hemolytic anemia/Evans syndrome by c-Myb. Int J Hematol 107: 666-672, 2018.
37. Fu Z, Li D, Jiang W, Wang L, Zhang J, Xu F, Pang D and Li D: Association of BTLA gene polymorphisms with the risk of malignant breast cancer in Chinese women of Heilongjiang province. Breast Cancer Res Treat 120: 195-202, 2010.
38. Sekar D, Govene L, Del Rio ML, Sirait-Fischer E, Fink AF, Brüne B, Rodriguez-Barbosa JI and Weigert A: Downregulation of BTLA on NKT cells promotes tumor immune control in a mouse model of mammary carcinoma. Int J Mol Sci 19: 752, 2018.